Aquaculture 564 (2023) 739031

Contents lists available at ScienceDirect

Aquaculture

journal homepage: www.elsevier.com/locate/aquaculture

Ectopic stem cell niches sustain rainbow trout (*Oncorhynchus mykiss*) intestine absorptive capacity when challenged with a plant protein-rich diet

Nicole Verdile [a], Gloriana Cardinaletti [b], Filippo Faccenda [c], Tiziana A.L. Brevini [d], Fulvio Gandolfi [a,*], Emilio Tibaldi [b]

[a] Department of Agricultural and Environmental Sciences, University of Milan, Italy
[b] Department of Agricultural, Food, Environmental and Animal Sciences, University of Udine, Italy
[c] Technology Transfer Centre, Edmund Mach Foundation, San Michele all'Adige (TN), Italy
[d] Department of Veterinary Medicine and Animal Sciences, University of Milan, Italy

ARTICLE INFO

Keywords:
Rainbow trout
Intestinal stem cell niche
Fish nutrition
Gut health
Vegetable proteins

ABSTRACT

To develop more sustainable feed formulations, it is important to assess in detail their effect on gut function and health. We previously described the specific organization of the epithelial and stromal components of the intestinal stem cell niche (ISCN), in rainbow trout (RT) under actual farming conditions. In the present work, we used our previous observation, for performing a comparative analysis between a control diet (CF) and an experimental vegetable-based diet (CV) under a new perspective. We correlated diet-induced changes of the morphology and the absorptive capability of the RT mucosa with modifications of the ISCN. Histological analysis confirmed that CV diet caused a mucosa remodeling, characterized by the generation of accessory branches sprouting from the middle of the proximal intestine folds, determining a significant increase of the luminal surface. The newly-formed structures showed positivity for PepT1, Sglt-1, and Fabp2 indicating their active role in small molecule absorption. However, the cells lining the base of the new branches expressed both epithelial (*sox9*) and stromal (*pdgfrα* and *foxl1*) stem cell markers, rather than the expected markers of fully differentiated cells. Our results suggest that a nutritional challenge results in the formation of an ectopic ISNC at the middle of the intestinal folds that sustains the formation of functional collateral branches, presumably to compensate for the reduced intestinal absorption. Overall, these data highlight, for the first time, the plasticity of the ISCN and its possible role in compensating intestinal functions in response to challenging conditions.

1. Introduction

The diet of intensively cultured salmonids has recently evolved with the reduction in the use of fish meals and oils in favor of more sustainable protein and lipid ingredients often of plant origin. Nonetheless, the presence of substantial levels of protein sources derived from plants and, in particular of soybean meal (SBM) in the diet represents a challenge to the fish welfare, as they are known to induce morpho-functional alterations in the digestive system, especially in the distal portion of the intestine (Baeverfjord and Krogdahl, 1996; Krogdahl et al., 2003; Refstie et al., 2000; Seibel et al., 2022). Recent investigations identified some of the anti-nutritional factors (ANFs) supplied by plant proteins that cause these alterations and provided further insight on their biological mechanisms and interactions with gut disorders (Abernathy et al., 2017; Blaufuss et al., 2020; Gaudioso et al., 2021; Pérez-Pascual et al., 2021). So far, the adverse effects of diets high in SBM and/or vegetable protein-rich derivatives have been investigated and described mostly based on classical histological parameters like folds shortening and branching, lamina propria widening, massive loss of enterocytes' vacuolization in the distal intestine (Li et al., 2019; Silva et al., 2015). However, these parameters are not directly linked to the specific mechanisms that control the proliferation of the intestinal epithelium and ensure its homeostasis in response to dietary challenges.

Indeed, the intestine is an extremely dynamic organ in which epithelial cells turnover occurs constantly and incessantly, preventing the passage of foreign antigens and other entities while, simultaneously promoting the absorption of useful molecules and nutrients (Barker, 2013; Beumer and Clevers, 2020; Giorgini et al., 2018). The proper balance between cell proliferation and differentiation is strictly controlled by a well-defined microenvironment called intestinal stem

* Corresponding author.
E-mail address: fulvio.gandolfi@unimi.it (F. Gandolfi).

https://doi.org/10.1016/j.aquaculture.2022.739031
Received 23 May 2022; Received in revised form 1 November 2022; Accepted 2 November 2022
Available online 6 November 2022

cell niche (ISCN) (Barker et al., 2008; Gehart and Clevers, 2019; Li and Clevers, 2010). This specific functional unit hosts a highly specialized population of tissue-resident stem cells known as intestinal stem cells that are physically and functionally connected with the underlying mesenchymal cells. The two cell populations interact to generate all the differentiated cell types and to preserve the stem cell reservoir through their balanced self-renewal (Li and Xie, 2005). Stem cell fate is driven by several growth and signaling factors mostly provided by a supportive mesenchymal cell population distributed along the peri-epithelial space (Aoki et al., 2016; Greicius et al., 2018). Experimental data demonstrated that ISCN components are highly susceptible to stressful and challenging conditions, making them a suitable and attractive target for evaluating the impact of alternative feeds on the intestinal mucosa, improving the sensitivity and the predictive power of current *in vivo* feeding trials (Heijmans et al., 2013; Verdile et al., 2019).

Recently we described the structure and organization of the intestinal stem cell niche in rainbow trout (RT, *Oncorhynchus mykiss*) (Verdile et al., 2020a), a widespread farmed fish species belonging to the *Salmonidae* family. Within the region of proliferating cells at the base of the folds, we identified and characterized a small group of epithelial cells selectively marked by the expression of the gene *sox9* that displays the morphological and ultrastructural features typical of the actively cycling intestinal stem cells. They are considered the corresponding functional equivalent of the so-called crypt-base columnar cells, the typical intestinal stem cells, extensively studied in mouse's intestine. Moreover, we integrated those results demonstrating that as it occurs in mice, also in RT, the epithelial components of the niche establish a direct connection with telocytes (TCs), a specialized supportive stromal cell population (Verdile et al., 2022).

This work is part of an extensive research whose results related to growth performances, gut health, microbiota composition and fillet quality have been previously reported (Bruni et al., 2021; Cardinaletti et al., 2022; Gaudioso et al., 2021; Randazzo et al., 2021). Here, we correlated diet-induced changes in the intestinal mucosa with those in the intestinal stem cell niche (ISCN) comparing Rainbow trout fed a diet that included soybean meal at a level known to cause adverse effects on gut health, and animals fed with a reference diet rich in fish meal and fish oil.

2. Material and methods

2.1. Ethics

The feeding trial experiment and all procedures involving animals were performed in accordance with the EU legal frameworks relating to the protection of animals used for scientific purposes (Directive 2010/63/EU). It was approved by the Ethics Committee of the Edmund Mach Foundation (n°99F6E.0) and the protocol was authorized by the Italian Ministry of Health (530/2018-PR).

2.2. Test diets

The experiment used two of the diets already described by Randazzo et al. (2021) whose ingredient composition, gross nutrient and energy contents are shown in Table 1.

A reference diet rich in fish derivatives, named CF was formulated to attain ratios between fish and vegetable protein and lipid sources of 90:10 and 80:20; respectively. A second preparation, named CV, inclusive of a substantial level of dehulled soybean meal (SBM), vegetable protein-rich derivatives and oils, was prepared to result in an opposite fish to vegetable protein and oil ratios than the CF one (i.e., 10:90 and 20:80, respectively). Both diets were formulated to be grossly isoproteic, isolipidic, isocaloric. Diet CV was supplemented with limiting amino acids, and both preparations were added with vitamins and minerals to fit all known nutrient requirements of rainbow trout (NRC, 2011). The diets were manufactured by SPAROS Lda. (Portugal) by extrusion in two pellet sizes (3 and 5 mm) and stored at room temperature, in a cool and aerated room while being used. The test diets were analyzed for moisture, ash, crude protein (N x 6.25) and phosphorus, according to AOAC (2016). Their lipid content was determined following Folch et al. (1957) (Folch et al., 1957). Gross energy was determined by adiabatic bomb calorimeter (IKA C7000, Werke GmbH and Co., Staufen, Germany). The analysis of amino acid composition of the test diets was performed using a HPLC system as described by Tibaldi et al. (2015) (Tibaldi et al., 2015). Acid hydrolysis with HCl 6 N at 115–120 °C for 22–24 h was used for all amino acids except cysteine (Cys) and methionine (Met), for which performic acid oxidation followed by acid hydrolysis was used and tryptophan, that was determined after lithium hydroxide (4 M) hydrolysis.

Table 1
Ingredient, proximate composition (%), gross energy and essential amino acid composition of the test diets.

	CF	CV
Ingredient composition		
Fishmeal[a]	47.5	–
CPSP 90[b]	5.0	5.0
SBM	–	23.0
Soy protein concentrate[c]		15.7
Wheat gluten	—	15.7
Rapeseed meal	3.8	3.5
Whole wheat	15.6	–
Pea meal	7.0	7.1
Fish oil	15.1	4.4
Rapeseed oil	3.8	9.3
Linseed oil	–	7.4
Palm oil	2.0	2.0
Vit & Min Premix[d]	0.2	0.2
Dicalcium Phosphate	–	3.0
Betaine HCl	–	1.5
L-Lysine	–	1.2
DL-Methionine		0.45
L-Tryptophan		0.05
Celite	1.5	1.5
Proximate composition (% as fed)		
Dry Matter	92.4	91.2
Crude protein	42.0	42.1
Crude lipid	23.9	23.9
Ash	9.5	8.0
Carbohydrates[*]	17.0	17.2
Gross Energy (MJ/kg)	22.4	21.9
Phosphorus (%)	1.33	0.69
Arg	2.4	2.6
His	0.9	1.0
Ile	1.6	1.7
Leu	2.6	2.9
Lys	2.9	2.9
Met + Cys	1.4	1.6
Phe + Tyr	3.1	3.3
Thr	1.6	1.4
Trp	0.5	0.4
Val	1.9	1.8

[a] Super Prime, Pesquera Diamante, San Isidro Lima, Peru.
[b] Fish protein concentrate, Sopropeche, Boulogne sur mer, France.
[c] Soy protein concentrate (Soycomil).
[d] Supplying per kg of supplement: Vit. A, 4000,000 IU; Vit D3, 850,000 IU; Vit. K3, 5000 mg; Vit.B1, 4000 mg; Vit. B2, 10,000 mg: Vit B3, 15,000 mg; Vit. B5, 35,000 mg; Vit B6, 5000 mg, Vit. B9, 3000 mg; Vit. B12, 50 mg; Vit. C. 40.000 mg; Biotin, 350 mg; Choline, 600 mg; Inositol, 150,000 mg; Ca, 77,000 mg; Mg. 20,000 mg; Cu, 2500 mg; Fe, 30,000 mg; I, 750 mg; Mn, 10,000 mg; Se, 80 mg; Zn, 10,000 mg.
[*] Carbohydrate calculated by difference as 100 – (Water + CP + Lipid + Ash).

2.3. Fish rearing conditions and tissue samples collection

The feeding trial was carried out at the aquaculture center of the Edmund Mach Foundation (S. Michele all'Adige, TN, Italy) using 300

rainbow trout of a local strain selected from a batch and distributed among 5 groups each consisting of 50 specimens, which were stocked in 1600 L fiberglass tanks supplied with well water (temperature 13.3 ± 0.03 °C; D.O. 7.4 ± 0.5 mg/l) by a flow-through system ensuring up to a total water volume replacement/tank/h. Each diet was fed to triplicate fish groups over 13 weeks. Fish were fed ad libitum by hand in two daily meals, 6 days a week. At the end of the feeding period, after 24 h fasting, the final fish biomass was recorded per each tank. All fish were subjected to anesthesia with tricaine methanesulfonate MS222 at dose of 100 mg/L (PHARMAQ, UK). The growth performance was evaluated by the increase in body weight (BW), daily feed intake (FI), specific growth rate (SGR) and feed conversion rate (FCR) as follows:

FI = average body weight/day; SGR = 100 × [(ln FBW-ln IBW)/days]; FCR = feed intake/biomass gain.

In addition, two fish per tank (6 for dietary treatment) were euthanized with an overdose of the same anesthetic at dose of 300 mg/L (PHARMAQ, UK). Fish were subjected to dissection by opening the ventral side of the animals to remove the gut. Small intestinal samples were cut from the proximal intestine, washed with a 0.9% saline solution to remove any content residue, fixed by immersion in 4% paraformaldehyde and stored at 4 °C for 24 h. Subsequently, samples were washed with MilliQ water and with 70% ethanol for 45 min and preserved overnight in a new 70% ethanol solution before performing the dehydration steps.

Proximal intestine has been selected as target region because it represents the predominant site where secretory and nutrient absorptive functions take place, ensuring for around 70% of the total nutrient absorption (Bjørgen et al., 2020). Accordingly, it shows higher expression of enterocytes' functional markers (Sglt1, PepT1 Fabp2) (Verdile et al., 2020a) compared to the distal intestine, making easier the identification even of subtle differences between the two dietary treatments.

2.4. Histology and histochemistry

Dehydration steps were performed by washing samples with a graded ethanol series (from 70 to 100%), followed by two final washing steps of 45 min each with the clearing agent Xylene (Bio-Clear, Bio-Optica, Milan, Italy). Samples were then embedded in liquid paraffin (Bio-Optica, Milano, Italy) at 55–58 °C. Formalin-fixed solidified paraffin blocks (FFPE) were then cut with a rotary microtome (Histoline MR2258, Milan, Italy) to obtain 5 μm sections that were stained with hematoxylin and eosin (HE) to evaluate sample morphology and to assess the eventual presence of inflammation signs. Alternatively, sections were stained with Alcian blue - Periodic acid – Schiff reagent (AB/PAS staining kit, Bio Optica, 04–163,802) to analyse the overall carbohydrates profile.

2.5. Immunohistochemistry and immunofluorescence

Peptide transporter 1 (PepT1), sodium-glucose transporter 1 (Sglt-1) and Fatty acid binding protein 2 (Fabp2) were selected as functional enterocytes' markers whereas proliferating cell nuclear antigen (*Pcna*) was used as marker of actively dividing cells. We previously validated antibodies specificity and reactivity in RT intestine (Verdile et al., 2020a). The specific distribution of PepT1, SglT1 and Pcna was characterized through indirect immunohistochemistry using the Avidin Biotin Complex method (VECTASTAIN® Elite® ABC, Vector Laboratories, Burlingame, CA, USA) following manufacturer instructions. Briefly, sections were brought to boiling in an antigen retrieval solution (10 mM sodium citrate buffer, 0.05% Tween20, pH 6 for PepT1 and Sglt-1, and 10 mM Tris-base, 1 mM EDTA solution, 0.05% tween20, pH 9 for *Pcna*) for 1 min. After cooling at room temperature, sections were incubated with 3% H_2O_2 solution in distilled water for 15 min to quench the endogenous peroxidase. Sections were then incubated in Normal Blocking Serum (Vectastain ABC Elite KIT, Burlingame, CA, USA) at room temperature for 30 min to prevent aspecific binding. Subsequently, slides were incubated with anti-PEPT1 mouse monoclonal antibody (Santa Cruz Biotechnology, sc-373,742, Heidelberg, Germany) diluted 1:100 in 4% BSA in PBS, with anti-SGLT-1 rabbit polyclonal antibody (Millipore Corporation, 07–1417, Darmstadt, Germany) diluted 1:10000 in 4% BSA in PBS, or with anti-PCNA Mouse monoclonal antibody (Millipore Corporation, MAB424, Darmstadt, Germany) diluted 1:1600 in 4% BSA in PBS for 60 min at room temperature in a humid chamber. Sections were then incubated with appropriate biotinylated secondary antibody for 30 min at room temperature in a humidified chamber followed by the avidin-biotinylated horseradish peroxidase (HRP) complex (Vectastain ABC Elite KIT, Burlingame, CA, USA) for another 30 min. Finally, sections were exposed to diaminobenzene (DAB) substrate (Vector Laboratories, SK-4105, Burlingame, CA, USA). Sections were then briefly counterstained with Mayer's hematoxylin, dehydrated and permanently mounted with a mounting media (Bio-Optica, 05-BMHM100, Milano, Italy). Fabp2 expression was detected through indirect immunofluorescence. Antigen retrieval was performed by incubating slides in a pressure cooker containing antigen retrieval solution (10 mM sodium citrate buffer, 0.05% Tween20, pH 6). Aspecific bindings were avoided by incubating slides in 10% donkey serum in PBS. Thereafter, samples were incubated with anti-FABP2 goat polyclonal antibody (Novus Biologicals, NB100–59746 Littleton, CO, USA) diluted 1:150 in 4% BSA in PBS for 60 min at room temperature in a humidified chamber. Subsequently, slides were incubated with the adequate secondary antibody Alexa Fluor™ 594 donkey anti-goat 1:1000 (Life Technologies Corporation, A11058 Willow Creek Road, OG, USA) for 30 min at room temperature. Sections were counterstained with 4,6-diamidino-2-phenylindole (DAPI) and mounted with ProLong™ Gold Antifade Mountant (ThermoFisher Scientific, Waltham, MA, USA). Secondary antibody controls were performed by omitting the primary antibody.

2.6. In situ hybridization

We previously selected SRY-Box 9 (*sox9*) as RT stem cell marker and Platelet Derived Growth Factor Receptor Alpha (*pdgfrα*) and Forkhead Box L1 (*foxl1*), as RT telocytes markers (Verdile et al., 2022). Here, we evaluated the alteration of spatial distribution of these stem cell niche components as a result of a fishmeal and fish-oil-based diet or a vegetable-based diet. *In situ* hybridization was performed using Multiplex Fluorescent Reagent Kit V2 (RNAscope technology, Advanced Cell Diagnostics, San Francisco, CA, USA) according to the manufacturer's indications as we previously described. In brief, FFPE sections of 5 μm were heated in a stove for 1 h at 60 °C and then immersed in xylene to promote paraffin removal. Samples were subsequently incubated with hydrogen peroxide (Advanced Cell Diagnostics, San Francisco, CA, USA) and brought to boiling in a target retrieval solution for 25 min (Advanced Cell Diagnostics, San Francisco, CA, USA). Thereafter, slides were exposed to Protease III (Advanced Cell Diagnostics, San Francisco, CA, USA) to encourage probes to reach their specific target. Afterward, sections were incubated with probes diluted 1:50 in diluent buffer in a HybEZ oven (Advanced Cell Diagnostics, San Francisco, CA, USA) for 2 h at 40 °C.

Signal amplification was performed by incubating samples in signal amplification solutions 1, 2, and 3. The signal was developed incubating slides with the appropriate fluorophore (OPAL 570, Akoya biosciences, Marlborough, MA, USA) diluted 1:750 in tyramide signal amplification (TSA) buffer. Sections were then counterstained with DAPI and mounted with ProLong Gold Antifade mountant (ThermoFisher Scientific, Waltham, MA, USA). The mRNA quality and integrity within FFPE samples were checked using a probe for a constitutive control gene (PPiB-Peptidylprolyl Isomerase B), while negative controls were performed by incubating slides with a probe specific for *Bacillus subtilis* dihydrodipicolinate reductase (dapB) gene.

2.7. Quantitative analysis

We quantified different aspects of the mucosal surface extension examining histological sections under a Zeiss AXION Zoom. V16 stereomicroscope equipped of a Axiocam 506 colour camera and the ZEN 2 version 2.0 package software or with a Leica DMR microscope equipped of a Nikon DS-Ri2 camera and the NIS-Elements D software, version 5.20. Images were observed at continuous magnifications between 6 and 400.

Hematoxylin-eosin stained sections of 3 individuals for each dietary treatment were used to measure the border between the submucosa and the tunica muscolaris while the extension of the absorptive surface was calculated tracing a continuous line along the epithelium lining the intestinal lumen. To compare measurements among individuals we normalized the extension of the absorptive surface with that of the submucosa (i.e. the extension of the folds surface originating from a given length of the intestinal wall).

Since we previously showed (Verdile et al., 2020a) that the stem cell niche is superimposed to the proliferating cells compartment identified by Pcna expression, we drew a line along the folds base in correspondence of $Pcna^{+}$ cells as a proxy to measure the stem cell niches extension. The length of the border between the submucosa and the tunica muscolaris was used to normalize the extension of the stem cell compartment among individuals. We also measured the ratio between $Pcna^{+}$ cells and the whole absorptive surface to evaluate the relationship between the extensions of the proliferating and the differentiated compartments. Examples of how the different measurements were taken, are shown in Fig. 1.

AB/PAS-stained sections were used to quantify the circumference of goblet cells' vacuoles. Three fish per diet were included in the analysis. 5 images per fish were randomly selected and all the visible vacuoles were quantified. Their circumference was estimated using the specific function of the open-source Qupath-0.2.3 software.

2.8. Statistical analysis

Statistical analysis has been performed using Student's *t*-Test. Data distribution and the homogeneity of variance has been assessed according to the Shapiro–Wilk normality test and Bartlett's test respectively. Differences has been considered statistically significant if $p < 0.05$.

Fig. 1. Representative image showing the sites of the measurements taken: a) length of the given tract of the intestinal mucosa measured at the interface between submucosa and tunica muscolaris; b) proliferating cells were measured drawing a line in correspondence of $Pcna^{+}$ cells as a proxy for evaluating the stem cell niches extension; c) the absorptive surface was measured tracing a line along the intestinal lumen.

3. Results

3.1. Growth performance

During the 13 weeks of the feeding trial, no mortality occurred, and the fish growth performance is shown in Table 2. The overall growth performance were just marginally and not significantly impaired in fish fed the CV diet, that tended to be lower in the final body weight and SGR values, and higher in the daily feed intake and FCR than fish fed the CF diet ($p > 0.05$).

3.2. Histological and histochemical analysis

Hematoxylin-eosin staining revealed that fish fed CF diet showed a physiological mucosal architecture. We observed the classical finger-like folds that protruded directly from the intestinal wall covered by a single columnar layer of regularly aligned epithelial cells, mainly composed by enterocytes with no vacuolization and actively secreting goblet cells. Conversely, the administration of the CV diet resulted in several morphological changes that included: folds that lost their typical finger-like shape and acquired a leaf-like phenotype, lamina propria widening, enterocytes' apical cytoplasm characterized by copious and well-defined supranuclear vacuolization (SNV), especially distributed at the folds apex. Leaf-like folds developed novel branches starting from the middle of the folds height; their surface was lined with a single layer of intact and functional epithelium mainly composed of enterocytes and mucin-secreting cells (Fig. 2 A-B).

Such an extensive remodeling of the mucosal surface resulted in a significant increase ($p < 0.01$) of the overall absorptive surface of the branched mucosa in fish fed with CV diet compared to that of the fish fed with the control diet (Fig. 2-C). On the contrary, goblet cells (GC) were abundant, and homogenously distributed along the epithelium of fish fed with both diets. In fact, their vacuoles' circumference did not differ between the two dietary treatments (Fig. 3).

AB/PAS staining revealed that the GC secretion was heterogeneous after both diets: most of them produced a mixed combination of acid and neutral mucins (AB and PAS-positive dark blue cells), while a few secreted either only neutral (PAS-positive magenta cells) or only acidic mucins (AB- positive light blue cells). However, only in fish fed with CV diet a supranuclear vacuolization was present in the apical portion of the enterocytes which were negative for PAS and showed a low affinity for AB, indicating the presence of an acid content (Fig. 4).

3.3. Functional enterocyte's markers

To assess whether the administration of a CV diet compromised the epithelium absorptive capacity, we analyzed the expression of three well-known enterocytes' functional markers: peptide transporter 1 (PepT1), sodium–glucose/galactose transporter 1 (Sglt-1-1), and fatty-acid-binding protein 2 (Fabp2), carriers of small peptides, glucose and galactose and fatty acids, respectively. Immunolocalization revealed that they were distributed along the enterocytes' brush border and in the apical part of the enterocyte's cytoplasm. The Fabp2 and Sglt-1 signal intensity was not influenced by the different diets (Fig. 5-6) whereas the

Table 2
Growth performance, daily feed intake (FI), specific growth rate (SGR) and feed conversion ratio (FCR) of rainbow trout fed the test diets over 13 weeks.

	CF	CV
Final weight (g/fish)	231.2 ± 7.7	227.9 ± 5.8
Feed Intake (g/kg ABW/d)	10.8 ± 0.1	11.0 ± 0.1
SGR	1.61 ± 0.02	1.57 ± 0.02
FCR	0.78 ± 0.02	0.80 ± 0.02

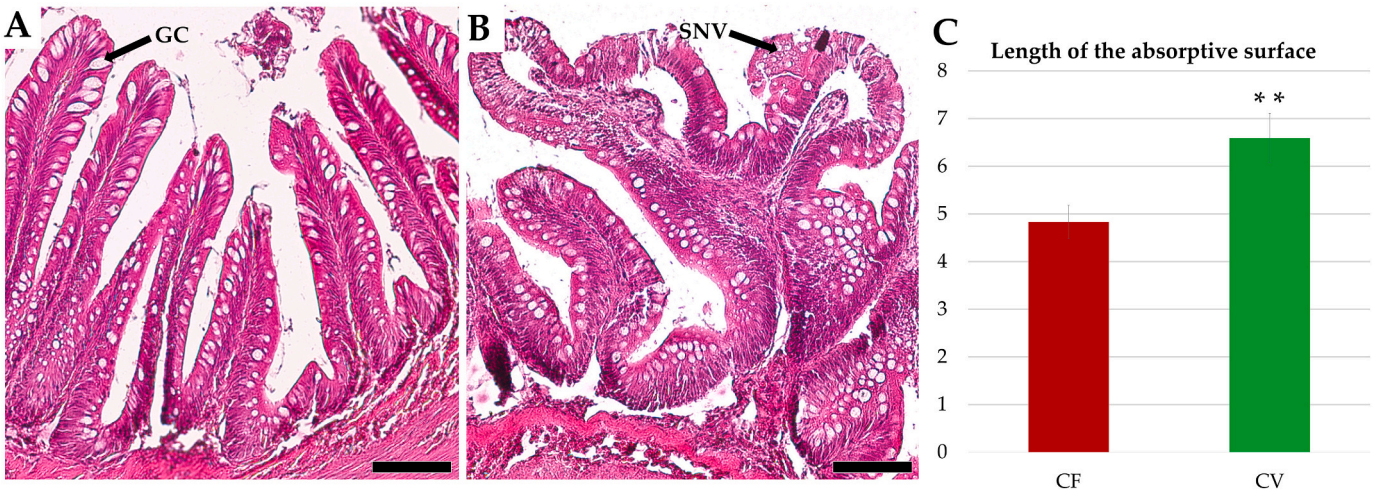

Fig. 2. Hematoxylin-eosin staining showing the physiological mucosa architecture of fish fed for 13 weeks with a fish based-diet (A) characterized by finger-like folds lined by a single layer of columnar cells composed by enterocytes and goblet cells (GC), and organization of the mucosa of fish fed with a vegetable-based diet (B) characterized by the presence of leaf-like folds from which novel accessory branches branch-off, lamina propria widening, and appearance of supranuclear vacuolization (SNV) in the apical portion of the enterocytes' cytoplasm. Scale bar 100 μm. (C) The extension of absorptive surface per unit of intestinal length is expressed as a ratio with the length of the intestinal tract and indicates that the branching formed following the administration of the CV diet significantly increases the luminal surface in fish fed with the CV diet. Values are expressed as mean ± SD. Differences were considered statistically significant if $p < 0.05$ (** indicate $p < 0.01$).

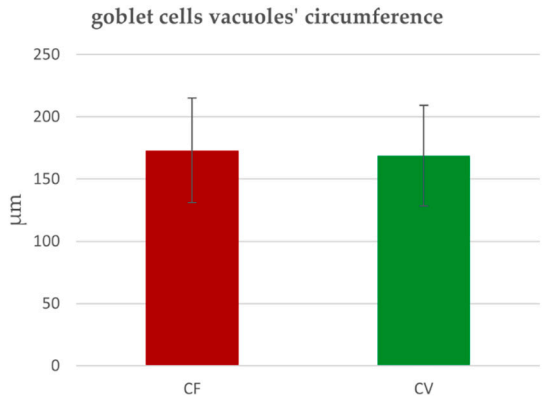

Fig. 3. Goblet cells vacuoles' circumference in fish fed for 13 weeks with CF or CV diet. Values are expressed as mean ± SD. Differences were considered statistically significant if p < 0.05 (no symbol indicate $p > 0.05$).

vegetable-based diet strongly inhibited the expression of PepT1 whose signal was restricted to the apical part of the enterocytes' cytoplasm as opposed to its homogenous distribution within the cytoplasm in fish fed diet CF (Fig. 7).

3.4. Proliferating cells

The two diets also affected the distribution of proliferating cells that were identified through the immunodetection of proliferative cell nuclear antigen (Pcna). As expected, cells were actively proliferating at the folds base in both experimental groups. In fish fed with a CF diet no proliferating cells were found along the folds length, confirming the presence of a fully differentiated compartment. On the contrary, $Pcna^+$ cells were found at the base of the novel branches that formed from the middle of the leaf-like folds height in fish fed with CV diet (Fig. 8).

Consistently with the increase of the absorptive surface described above in fish fed with the CV diet, the extension of the $Pcna^+$ epithelial cells was also higher than in fish fed with CF diet (Fig. 9-a). However, that ratio between differentiated and proliferating epithelial cells remained the same in both diets (Fig. 9-b).

3.5. Effect of a vegetable-based diet on the epithelial and the stromal components of the stem cell niche

The diet had no effect on the localization of cells expressing high level of *sox9* that are the functional equivalent of mouse CBC cells, the *bona fidae* intestinal stem cells (Fig. 10). These cells were restricted at the base of the folds where the stem cell compartment is found. However, in animals fed with the CV diet we observed slender and elongated stem cells expressing *sox9* at high levels also at the base of the newly formed branches (Fig. 11).

Pdgfrα positive cells were in the lamina propria, the connective layer just underneath the epithelial cells, irrespectively of the diet. We could identify two different $pdgfr\alpha^+$ populations: one expressed *pdgfrα* at a high level identifying them as telocytes, regularly aligned along the basement membrane, and creating a complex mesh extended all the way from the base to the tip of the folds (Fig. 12). The other expressed *pdgfrα* at lower level and was found deeper in the lamina propria. Interestingly, in fish fed with the CV diet, telocytes formed a supportive network also in correspondence to the points where the newly formed branches emerged in the proximal intestine (Fig. 13).

The presence of *foxl1*-expressing telocytes in the peri-epithelial space encircling the folds' base was also not influenced by the diet (Fig. 14-15). However, in the proximal intestine of fish fed with a CV diet, *foxl1*-expressing telocytes cells were found not only surrounding the folds' base but also around the base of the accessory branches departing from the mid of the fold height (Fig. 15).

Immunolocalization of Pcna revealed that telocytes enwrapping the folds' base were not proliferating neither in fish fed with a CF diet nor when the CV diet was administrated (Fig. 16). The same was true for the telocytes encircling the base of the newly formed branches in fish fed with a CV diet (Fig. 17).

4. Discussion

We previously characterized the epithelial cells lining the rainbow trout (RT) intestinal mucosa (Verdile et al., 2020b) and the specific organization of the intestinal stem cell niche in animals reared in actual farming conditions (Verdile et al., 2020a). In the present study, based on our previous results, we correlated the changes induced by a challenging

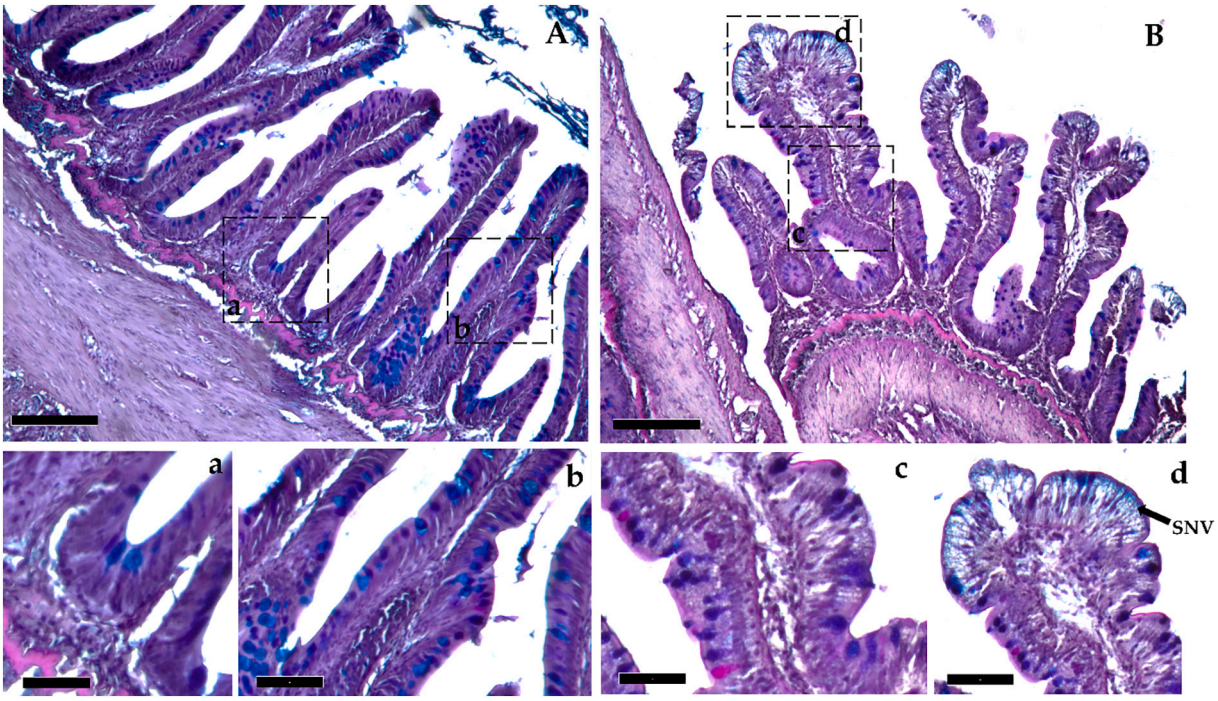

Fig. 4. Alcian Blue–Periodic acid–Schiff (AB-PAS) stained section showing the presence of a qualitatively heterogenous populations of goblet cells in both fish fed for 13 weeks with a CF (A-scale bar 250 μm) or CV diet (B-scale bar 250 μm). Most of them produced a mixed secretion (PAS-AB positive-dark blue cells), whereas only few of them secreted only acid mucins (AB positive-light blue cells) or neutral mucus (PAS positive-magenta cells) (photomicrographs a-b-c, (a-c scale bar 50 μm, b-scale bar 100 μm). SNV (arrow) that appeared in the proximal intestine of fish fed with a CV diet displayed an acidic content (d-scale bar 50 μm). (For interpretation of the references to colour in this figure legend, the reader is referred to the web version of this article.)

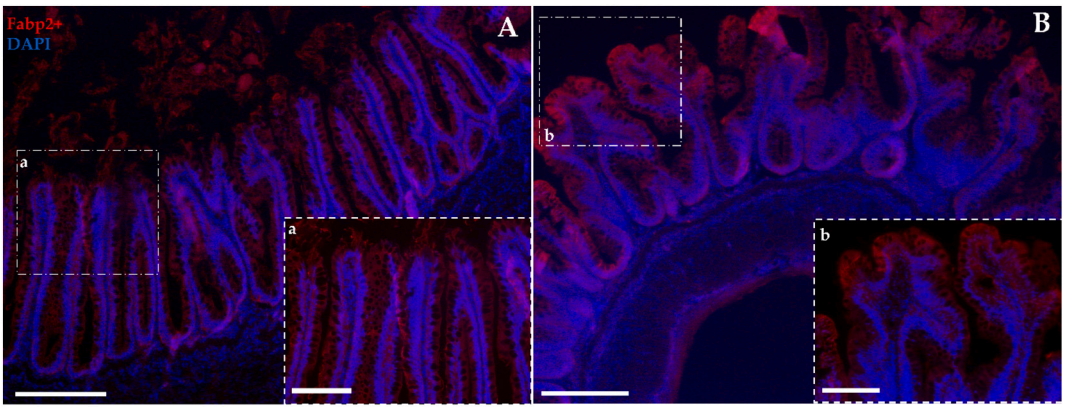

Fig. 5. Immunolocalization of Fabp2 in the proximal intestine of rainbow trout fed for 13 weeks with CF (A) or CV (B) diet (Scale bar 250 μm). A strong enterocytes' cytoplasmic signal with an increasing gradient from the base of the fold towards their tip was observed irrespectively of the diet (a- scale 100 μm). Moreover, a considerable Fabp2 expression was detected also in the epithelium lining the branches that originated from the regular mucosa folds of fish fed with the CV diet (b-scale 100 μm). Nuclei are counterstained with DAPI.

vegetable-based diet on the intestinal morphology and function with the effects on the RT intestinal stem cell niche.

Microscopically, the proximal intestinal mucosa of fish fed with the reference diet (CF) showed the typical physiological mucosa architecture, with finger-like folds, covered by an epithelium composed of many enterocytes with no vacuolization and quite a few active mucin-secreting goblet cells. Conversely, the mucosa of fish fed with a CV diet showed the equally typical inflammatory signs extensively described in salmons (*Salmo salar*) affected by the soybean meal enteritis (Krogdahl et al., 2015). These included folds that lost their distinctive finger-like shape and acquired a peculiar leaf-like phenotype, occurrence of numerous supranuclear vacuolization of the enterocytes' cytoplasm, lamina propria widening, and generation of novel branches starting from the middle of the folds. These newly-formed structures were lined by an intact epithelium, and exactly as the common folds protruding from the intestinal wall, were defined by a single columnar layer of enterocytes and scattered goblet cells.

The quantitative analysis demonstrated that the mucosa branching observed in fish fed with the CV diet determined a significant increase of the absorptive surface. Intriguingly, the expansion of the absorptive surface when something threatens the mucosa integrity is quite uncommon. Indeed, it has been recently well documented that perturbation of mouse intestinal mucosa results in rapid loss differentiated cells that, in turn, causes temporarily villus atrophy impairing nutrient absorption (Ohara et al., 2022). Instead, the fact that RT is able to develop an efficient regenerative response to compensate for the effect of a

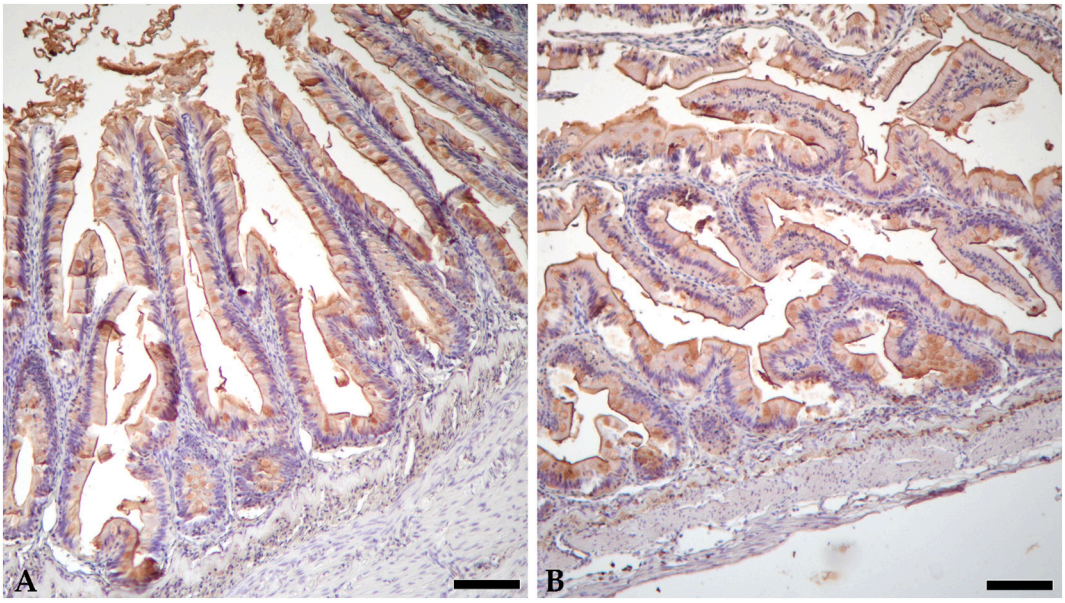

Fig. 6. Representative images showing immunolocalization of Sglt-1 in the proximal intestine of rainbow trout fed for 13 weeks with CF (A) or CV (B) diet. Sglt1 was distributed along the enterocytes brush border with no remarkable differences between the two dietary treatments. (Scale bar 100 μm).

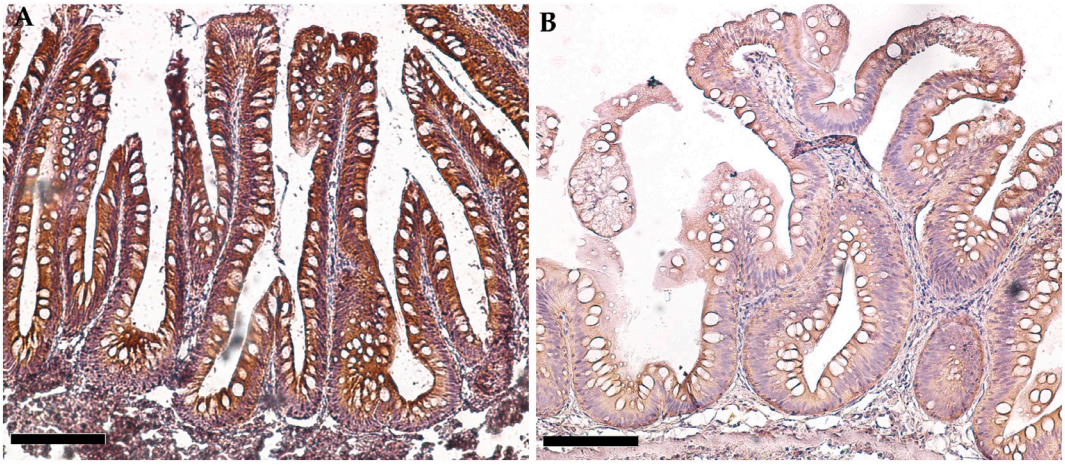

Fig. 7. Immunolocalization of PepT1 marker in the proximal intestine of fish fed for 13 weeks with a CF (A) and CV (B) diet. A strong PepT1 signal was observed along the enterocytes' brush border and in the apical portion of the enterocytes' cytoplasm of fish fed with a CF diet, whereas only a weak expression was found in epithelial cells of fish fed with a CV diet (Scale bar 100 μm).

stressful event, could be explained as a sort of evolutionary phenomenon, since lower organisms are capable to regenerate partially or totally their digestive system (Forsthoefel et al., 2011).

Goblet cells were abundant, and uniformly distributed along the epithelium lining the mucosa of fish fed with both diets with no significant differences between the two groups. Their secretion was qualitatively heterogenous since most of them produced a mixed combination of complex carbohydrates, as previously described in rainbow trout and other teleost species (Banan Khojasteh et al., 2009; Elia et al., 2018; Hamidian et al., 2018; Verdile et al., 2020b) also in the distal intestine. Feeding the animals with the CV diet induced the formation of supranuclear vacuoles with an acidic content, in the apical portion of the enterocytes. Supranuclear vacuoles are abundant and commonly observed in the distal intestine of several fish species, including RT, where they contain neutral PAS-positive granules because of whole protein uptake and indicate normal intestinal activity (Antoni et al., 2006). On the contrary, the appearance of supranuclear vacuoles with an acidic content has not been reported before and requires further investigations to understand its functional implication.

We studied the absorptive capability of the intestinal epithelium through the immunolocalization of three well-known enterocytes' functional marker. The first, peptide transporter 1 (PepT-1), is a transmembrane transporter that selectively regulates the uptake of di- and tripeptides across the enterocytes' brush borders in mammals (Wenzel et al., 2001) and fish (Wang et al., 2017). Previous observation in RT (Ostaszewska et al., 2010; Verdile et al., 2020a), salmon (Romano et al., 2014), sea bass (Terova et al., 2009) and sea bream (Terova et al., 2013) indicate that PepT-1 transcripts are abundant in the proximal intestine and pyloric caeca, whereas its expression steadily decreased moving towards the distal intestine. In this experiment, we observed an intense PepT-1 signal in the enterocyte's brush border and in the apical part of the cytoplasm of fish fed with CF diet. On the contrary, only a weak expression was detected in fish fed with CV diet along the epithelium of both common folds and newly-generated branches. This suggests that the substitution of the marine protein sources with plant-based raw materials compromises the ability of the intestine to internalize small

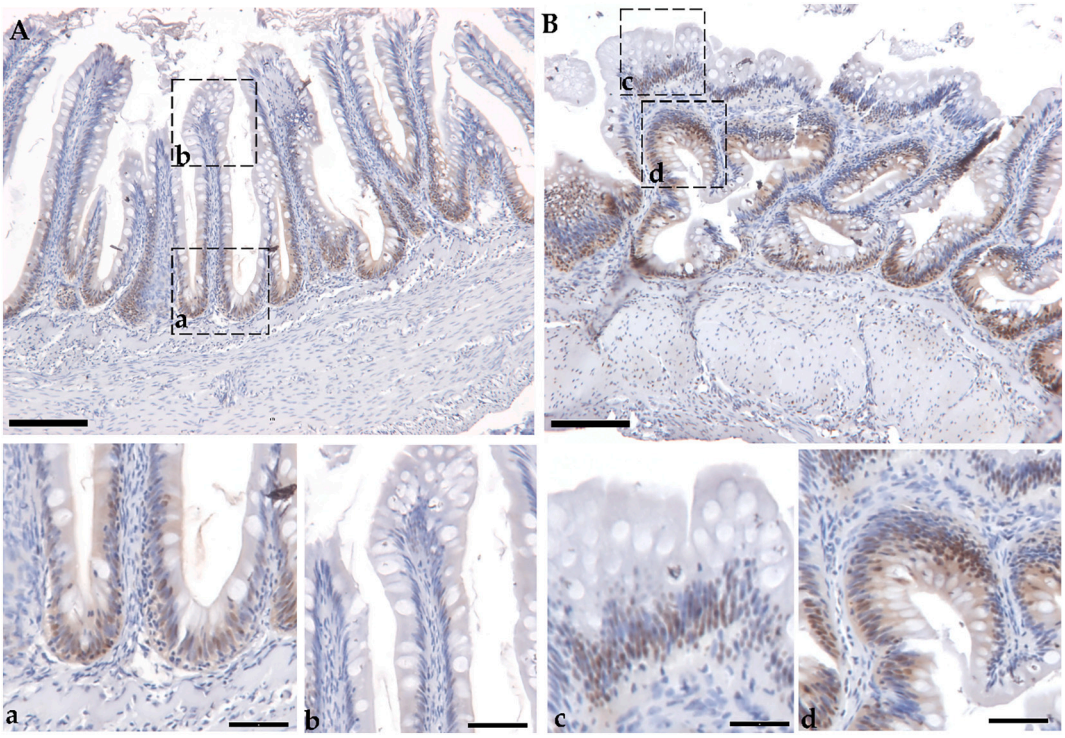

Fig. 8. Representative images showing the distribution of proliferating cells in the proximal intestine of rainbow trout fed for 13 weeks with a CF (A) or a CV (B) diet though the immunolocalization of proliferating cell nuclear antigen (Pcna) marker (Scale bar 250 μm). $Pcna^{+}$ cells were confined to epithelial cells nuclei lining folds base in both fish fed with a CF or a CV diet (a- Scale bar 50 μm). No $Pcna^{+}$ cells were found along the folds length (b-Scale bar 50 μm), outside of the proliferative compartment in fish fed with a CF diet. On the contrary, spotted of $Pcna^{+}$ cells were found outside the folds base and in correspondence of the novel generated branches in fish fed with a CV diet (c-d- scale bar 25 μm).

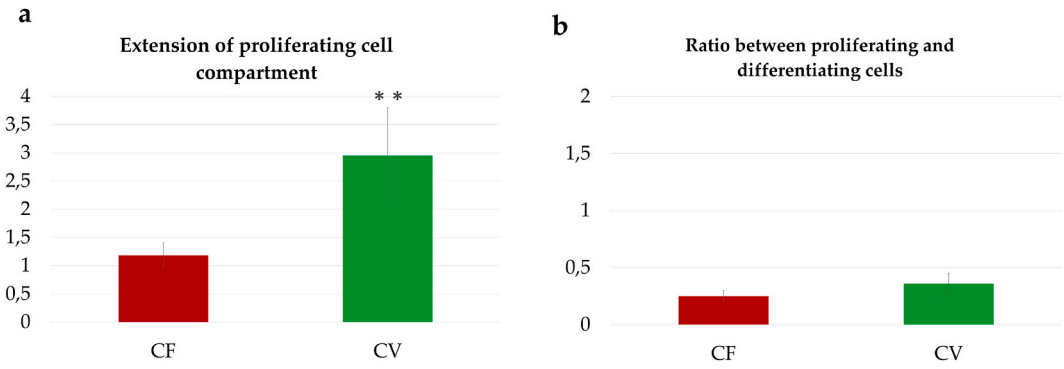

Fig. 9. (a) the increase in the absorptive surface described in fish fed for 13 weeks with CV diet was also accompanied by a significant increase of the proliferating cell compartment; (b) however the ratio between proliferating and differentiated cells remained constant in the two diets. Values are expressed as mean ± SD. Differences were considered statistically significant if $p < 0.05$ (** indicate $p < 0.01$).

peptide across the brush border. The decrease of PepT1 expression that we documented, is consistent with previous studies performed in European sea bass (Terova et al., 2009) and sea bream (Terova et al., 2013) in which it has been demonstrated that the dietary inclusion of vegetable-based protein, lead to a downregulation of PepT-1 expression. Moreover, the limited expression of PepT-1 in sea bream also correlated with a significant reduction of the fish growth performances (Terova et al., 2013). However, in our case the reduced expression and distribution of PepT1 did not result in a reduced body weight and a lower SGR (Cardinaletti et al., 2022; Randazzo et al., 2021). A possible explanation for this observation could be that the limited PepT-1 expression was compensated by the significant increase of the absorptive surface that we measured in fish fed with CV diet and thus the presence of a higher number of epithelial cells expressing this transmembrane protein.

The second enterocyte functional marker, the fatty acid binding protein 2 (Fabp2), mediates the intercellular transport of long-chain fatty acids across the enterocyte membrane. In addition, since the administration of a plant-based meal to salmonids species causes intestinal mucosa inflammation and is often correlated with a significant reduction of lipid digestibility, Fabp2 also represents a valuable indicator of the correct intestinal function and of general gut health (Venold et al., 2012). Immunolocalization of Fabp2 showed a strong enterocytes' cytoplasmic signal with an increasing gradient from the base of the fold towards their tip, irrespectively of the diet. Moreover, a considerable Fabp2 expression was detected also in the epithelium lining the branches that sprouted from the regular mucosa folds of fish fed with the CV diet. This finding is partially in contrast with the significant reduction of both Fabp2 transcriptional and protein levels described in

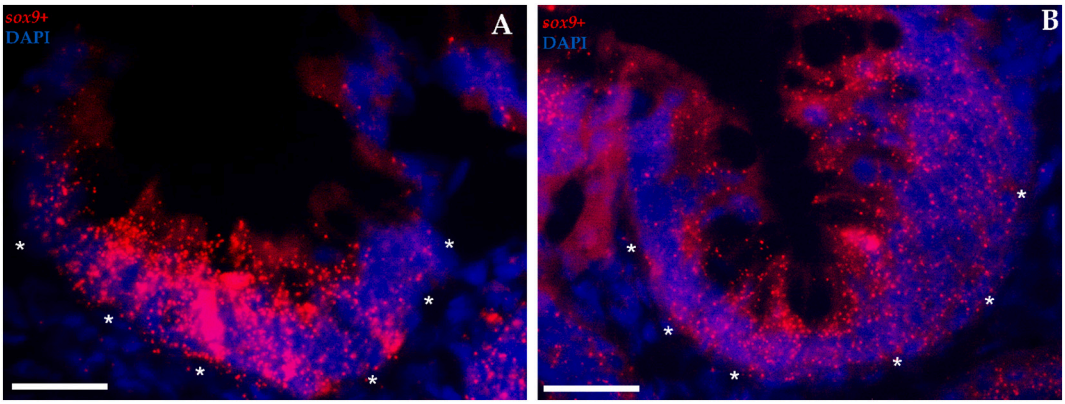

Fig. 10. *In situ* hybridization of *sox9* mRNA cells (red dots) in the proximal intestine of fish fed for 13 weeks with a CF (A) or a CV (B) diet. *Sox9*+ cells were observed confined to the stem cell zone in the epithelium lining the folds base irrespectively of the administrated diet (Scale bar 50 μm). Nuclei are counterstained with DAPI. Asterisks indicate the boundary between epithelium and connective tissue. (For interpretation of the references to colour in this figure legend, the reader is referred to the web version of this article.)

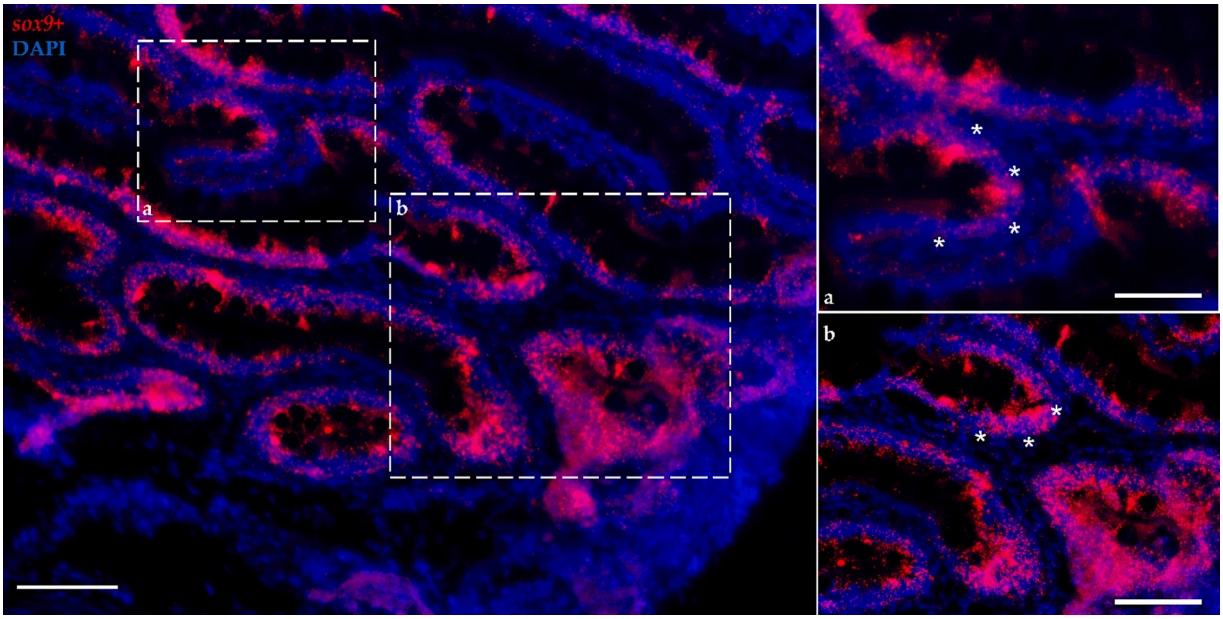

Fig. 11. *In situ* hybridization of *sox9* mRNA (red dots) in the proximal intestine of fish fed for 13 weeks with CV diet (scale bar 250 μm) showing the presence of *sox9*$^{+}$ cells at base of the mucosa folds (b- scale bar 100 μm) as well as in correspondence to the bases of the novel accessory branches that originate from the middle of the folds height (a- scale bar 50 μm). Nuclei are counterstained with DAPI. Asterisks indicate the boundary between epithelium and connective tissue. (For interpretation of the references to colour in this figure legend, the reader is referred to the web version of this article.)

Atlantic salmon fed with soybean meal (Venold et al., 2013). A possible explanation could be that different RT strains have diverse sensitivity to dietary soybean meals with regard to intestinal inflammation, enterocytes proliferation, and expression and distribution of Fabp2 (Venold et al., 2012).

We also evaluated the expression and the distribution of Sglt-1, a key mediator of glucose and galactose across the brush border membrane. In mammals, glucose represent the essential source of energy making it fundamental for the maintenance of homeostasis (Polakof and Soengas, 2013). Although we did not record relevant differences of Sglt-1 expression between the two dietary treatments, it is important to note that the accessory branches developed from the mucosa of fish fed with a CV diet also showed positivity for Sglt1.

Overall, our results indicate that the branched folds developed in response to the CV diet were morphologically similar to the regular folds. Their presence determined a significant increase of the mucosal surface and together with a diminished expression of PepT-1 suggests that the mucosa of fish challenged with a vegetable-based diet, compensates for an altered absorption efficiency by increasing the epithelial surface. However, the fact that the expression of carrier proteins involved in lipids and carbohydrates absorption was not affected also suggests that their function is regulated through specific mechanisms that are not related with the extension of the luminal surface.

The intestinal epithelium undergoes a high turnover rate and damaged cells are constantly replaced. In all species, the renewal mechanisms are driven by a specialized population of stem cells, located in a niche, that generates a pool of highly proliferating cells that, in turn, will differentiate into specific functional cell types. Given its fundamental role, this sophisticated and well-defined microenvironment is known to be susceptible to stressful and challenging conditions affecting the intestinal mucosa (Bankaitis et al., 2018; Verdile et al., 2019). Therefore, we investigated, for the first time, the diet-induced changes on the stem cell niche in a fish species.

As expected, proliferating - Pcna^{+} – cells were restricted to the

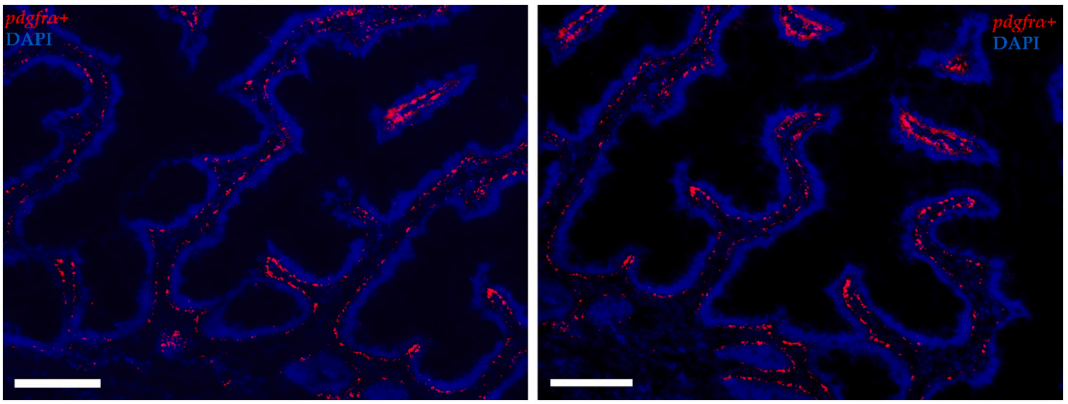

Fig. 12. *In situ* hybridization of *pdgfrα* mRNA (red dots) in the proximal intestine of fish fed for 13 weeks with a CF diet. *Pdgfrα* expressing subepithelial telocytes, generated a supportive network extending from the folds base towards their tips. (A- scale bar 100 μm, B- 50 μm). Nuclei are counterstained with DAPI. (For interpretation of the references to colour in this figure legend, the reader is referred to the web version of this article.)

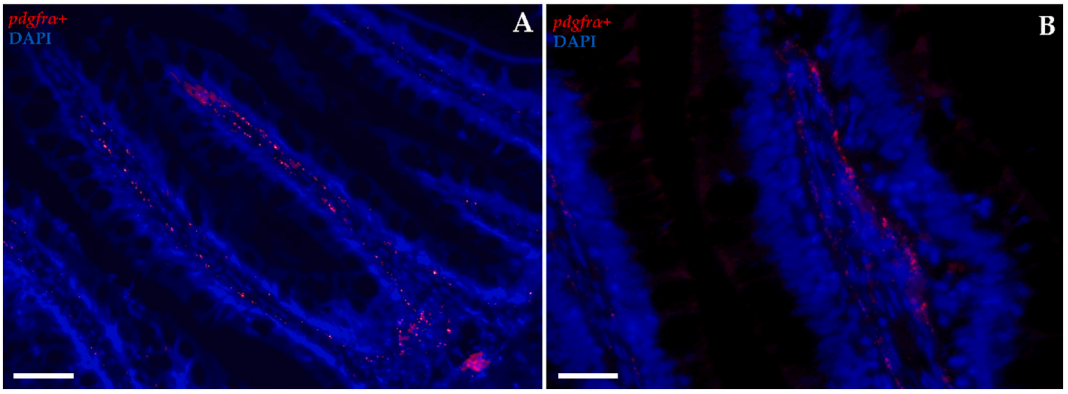

Fig. 13. *In situ* hybridization of *pdgfrα* mRNA (red dots) in the proximal intestine of fish fed for 13 weeks with a CV diet. Interestingly, in fish fed with the CV diet, *pdgfrα* expressing subepithelial telocytes, created a supportive network extending from the folds base towards their tips following the mucosa remodeling (Scale bar 250 μm). Nuclei are counterstained with DAPI. (For interpretation of the references to colour in this figure legend, the reader is referred to the web version of this article.)

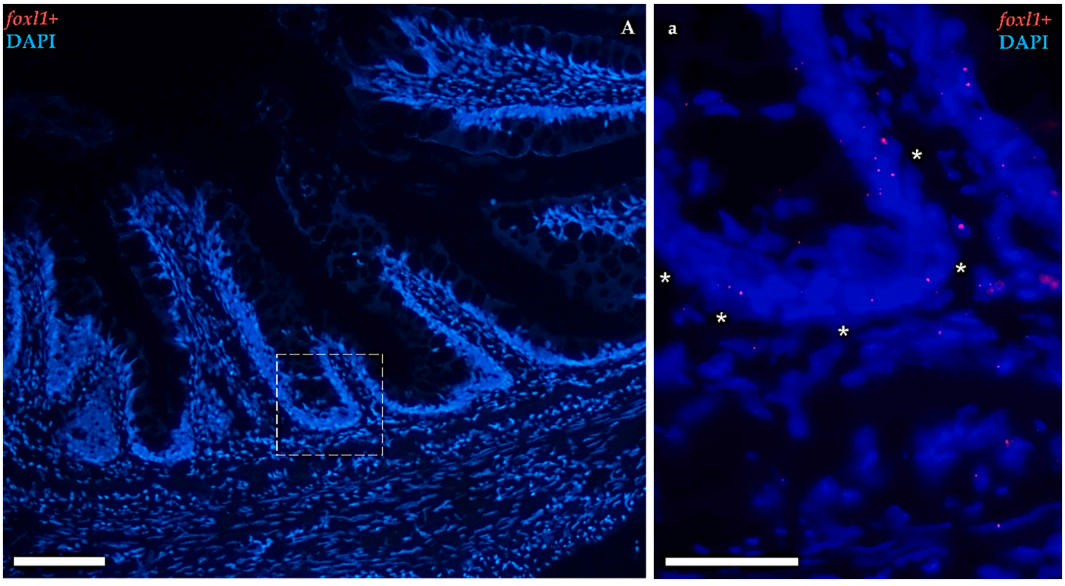

Fig. 14. *In situ* hybridization of *foxl1* mRNA dots (red dots) in the proximal intestine of fish fed for 13 weeks with CF diet showing the distribution of *foxl1*$^{+}$ cells encircling folds base. Nuclei are counterstained with DAPI (A-scale bar 250 μm, a-scale bar 25 μm) (asterisks indicate the boundary between epithelium and connective tissue). (For interpretation of the references to colour in this figure legend, the reader is referred to the web version of this article.)

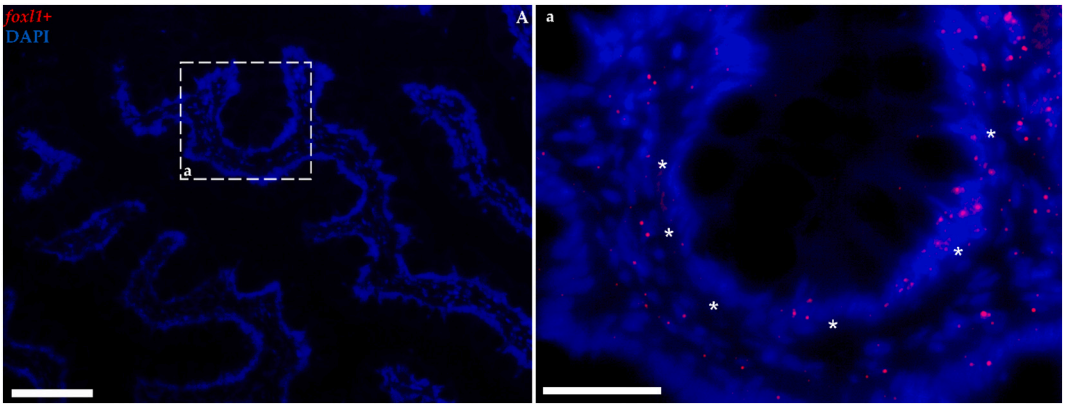

Fig. 15. *In situ* hybridization of *foxl1* mRNA (red dots) in the proximal intestine of fish fed for 13 weeks with CV diet showing the distribution of *foxl1*+ cells encircling the base of the novel generated branches started from the middle of the folds heigh. Nuclei are counterstained with DAPI (A-scale bar 250 μm, a-scale bar 25 μm) (asterisks indicate the boundary between epithelium and connective tissue). (For interpretation of the references to colour in this figure legend, the reader is referred to the web version of this article.)

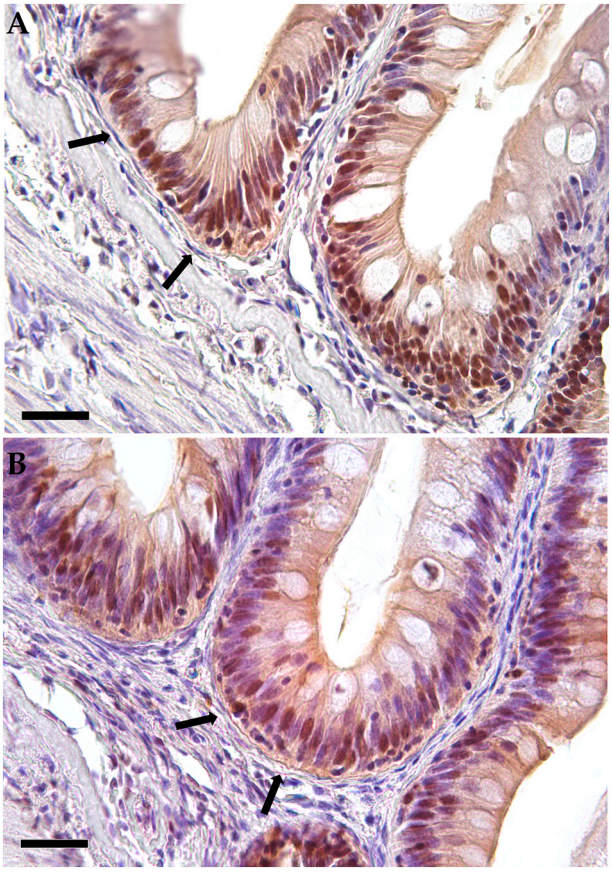

Fig. 16. Immunolocalization of proliferating cell nuclear antigen (Pcna) in fish fed for 13 weeks with a CF (A) or CV diet (B). A strong signal was observed in the epithelial cell nuclei located at the folds base irrespective of the administrated diet. Subepithelial telocytes encircling the proliferative zone did not show expression (arrows, scale bar 25 μm)

epithelium lining the folds' base in fish fed with both diets, further confirming the presence of a well-defined proliferating compartment. Previously, we observed that few Pcna$^+$ cells become visible along the fold's length in RT displaying mild inflammation signs (Verdile et al., 2020b). At the time, we speculated that these spots could correspond to the emerging points of the novel branches. Our hypothesis seems to be confirmed by the presence of small groups Pcna$^+$ cells at the base of the branches that formed from the leaf-like folds of the mucosa of fish fed with the CV diet. Furthermore, we observed that the extension of proliferating cells was significantly wider in CV fed fish than in the control group. This is not surprising since we previously observed that Pcna$^+$ cells largely overlap with the stem cell compartment (Verdile et al., 2020a), suggesting the formation of novel stem cell niches scattered in the remodeled mucosa. Interestingly, the ratio between proliferating and differentiated cells in challenging conditions remained the same as in the control treatment, suggesting that the intestinal mucosa was undergoing a controlled proliferation maintaining an optimal ratio between the two compartments. We characterized the specific organization of the RT stem cell niche (Verdile et al., 2020a), identifying *sox9* as the bona *fidae* intestinal stem cell marker in RT. Indeed, *sox9*$^+$ cells are limited to the epithelial cells lining the folds' base and display the distinctive features described for mouse intestinal stem cells (Barker et al., 2007). We also investigated the organization of the stromal component and identified a specialized fibroblast population, the telocytes, as the stromal cells involved in both short and long-range cell-to cell communication (Verdile et al., 2022). In this set of experiments, *sox9*$^+$ cells were observed in the epithelium lining the folds' base of fish fed with both CF and CV diet, further confirming the existence of a well-defined functional stem cell unit. However, *sox9*$^+$ cells were also found lining the base of the newly formed branches along the mucosa of fish fed with the CV diet. The interesting aspect is that the newly-formed branches originated from the mid of the folds height, therefore in the middle of the fully differentiated compartment and consequently completely outside of the stem cell zone. Recent experimental data conducted in mouse demonstrated that some terminally differentiated cells, in response to tissue perturbation or injuries, revert to a complete stem-like state (Hageman et al., 2020; Liu and Chen, 2020; Tata et al., 2013), generating *Lgr5*$^+$ cells, the well-established actively cycling stem cells in mouse intestine and equivalent to the *sox9*$^+$ cells in RT (Verdile et al., 2020a). In a recent work, Tetteh et al. (2016) induced *Lgr5*$^+$ cells ablation through the injection of diphtheria toxin and demonstrated that alkaline phosphates-expressing enterocytes were able to completely revert their phenotype into *Lgr5*$^+$ crypt stem cells. Based on these findings, the authors supposed that the typical one-way hierarchy valid for most adult stem cells seems not to be applicable to intestinal tissues in which differentiated cells, if required, are capable to de-differentiate their terminal phenotype to a multipotent state. This process has been already observed in other epithelial tissue like the mature airway cells in the mouse lung (Tata et al., 2013), and in Troy$^+$ chief cells in the gastric corpus of the same species (Guo et al., 2014). Enterocyte plasticity could be associated with a permissive epigenetic state of their precursors', since it seems that the distinctive chromatin arrangement, typical of the

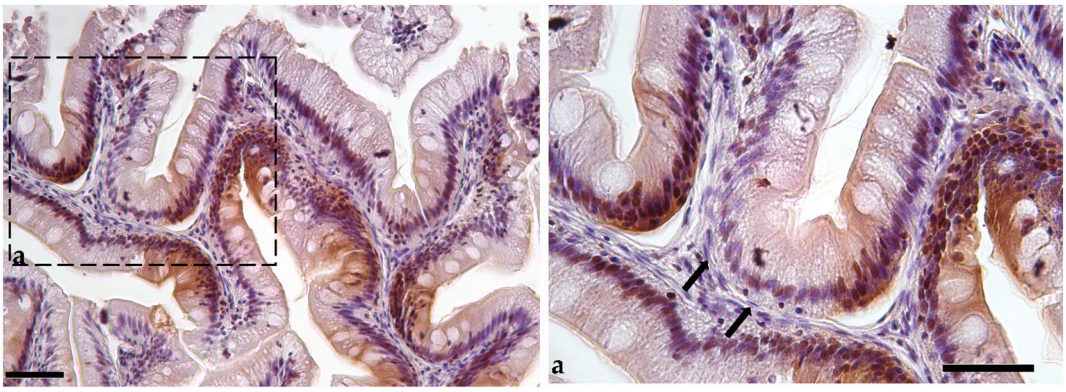

Fig. 17. Immunolocalization of proliferating cell nuclear antigen (Pcna) in fish fed for 13 weeks with a CV diet (Scale bar 100 μm). A strong signal was observed in the epithelial cell nuclei located at the base of the folds of the novel generated branches. On the contrary, subepithelial telocytes enwrapping the newly-formed proliferative compartments did not show expression (arrows-a, scale bar 25 μm).

enterocytes' precursors, is physiologically predisposed to be reprogrammed to generate *Lgr5*$^{+}$ cells (Tetteh et al., 2016). Similarly, it has been documented that Paneth cells, a differentiated secretory cell population located within the crypt base in mouse intestine, as well as enterocytes precursors distributed in the upper part of the crypt are able to revert their state to reconstitute the stem cells reservoir upon ISCs loss (Bohin et al., 2020; Chen et al., 2018; Mei et al., 2020; Pentinmikko and Katajisto, 2020; Van Es et al., 2012). Although we were not able to verify the de-differentiation processes of mature enterocytes' into *sox9*$^{+}$ cells since gene ablation and lineage tracing studies are unfeasible in RT, the fact that we observed novel *sox9*$^{+}$ cells in the typical location of fully differentiated enterocytes', far from the common stem cell zone, suggests that a similar process could also take place in RT intestine when something threats intestinal mucosa integrity. Interestingly, these *sox9*$^{+}$ cells give rise to accessory branches that act as fully functional units being supplied with an intact epithelium.

Telocytes are specifically distributed along the intestinal stroma just below the enterocytes' basement membrane (Verdile et al., 2022). With their characteristic small, nucleated cell body and their variable number of extremely long and thin processes, telocytes create an extended mesh spanning from the fold base to its tip that provides the essential signals ensuring the proper barrier integrity and homeostasis. We observed that *pdgfrα*$^{+}$ and *foxl1*$^{+}$ telocytes were precisely aligned below the epithelial cells at the base of the newly created branches. Indeed, telocytes possess essential homing properties that allow their optimal distribution immediately below the epithelial tissues (Nicolás et al., 2021). *FOXL1*$^{+}$ telocytes form a subepithelial plexus that extends from the stomach to the colon. This network produces and compartmentalizes Wnt ligands and inhibitors, thereby creating the physiological gradient that regulates an orderly differentiation (Shoshkes-Carmel et al., 2018). Furthermore it has been recently shown that mouse intestinal PDGFRα^{+} stromal progenitors is required for postnatal intestinal epithelial maturation and spatial organization (Jacob et al., 2022). All this suggests that the formation of the new branches is supported by the rearrangement of the mesenchymal component of the niche ensuring the appropriate differentiation of the epithelium overhead.

In conclusion, we observed a correlation between the formation of accessory branches sprouting from the intestinal folds of the anterior intestine and the appearance of ectopic ISCN in response to the nutritional stress induced by the CV diet. The quantitative analysis showed that folds branching leads to a significant increase of the absorptive surface and, in parallel, of the proliferating cells. Interestingly the ratio between proliferating and differentiated cells remains constant. To the best of our knowledge this is the first evidence suggesting how the ISCN contributes to the maintenance of RT intestinal mucosa homeostasis in response to a challenging diet.

Declaration of Competing Interest

The authors declare no conflicts of interest, financial or otherwise.

Data availability

Data will be made available on request.

Acknowledgment

This work was supported by the European Union's Horizon 2020 research and innovation program under grant agreement No 828835 and by SUSHIN (SUstainable fiSH feeds INnovative ingredients) project funded by Ager (AGER2-SUSHIN Cod 2016–0112).

Nicole Verdile, Tiziana A.L. Brevini and Fulvio Gandolfi are members of COST Action 16,119 and MIND FoodS HUB (Milano Innovation District Food System Hub).

References

Abernathy, J., Brezas, A., Snekvik, K.R., Hardy, R.W., Overturf, K., 2017. Integrative functional analyses using rainbow trout selected for tolerance to plant diets reveal nutrigenomic signatures for soy utilization without the concurrence of enteritis. PLoS One 12. https://doi.org/10.1371/journal.pone.0180972.

Antoni, Przybyb, Teresa, Ostaszewska, Mazurkiewicz Jan, W.A., 2006. The effect of experimental starters on morphological changes in the intestine and liver of common carp (*cyprinus Carpio L.)* larvae reared under controlled conditions. Arch. Polish Fish. 14, 67–83.

AOAC, 2016. Official Methods of Analysis of the Association of Official Analytical Chemists. In: George, W., Latimer Jr., A.A.V.V. (Eds.), 20th. Washington DC, USA. ISBN 0-935584-87-0.

Aoki, R., Shoshkes-Carmel, M., Gao, N., Shin, S., May, C.L., Golson, M.L., Zahm, A.M., Ray, M., Wiser, C.L., Wright, C.V.E., Kaestner, K.H., 2016. Foxl1-expressing mesenchymal cells constitute the intestinal stem cell niche. Cmgh 2, 175–188. https://doi.org/10.1016/j.jcmgh.2015.12.004.

Baeverfjord, G., Krogdahl, Å., 1996. Development and regression of soybean meal induced enteritis in Atlantic salmon, *Salmo salar* L., distal intestine: a comparison with the intestines of fasted fish. J. Fish Dis. 19, 375–387. https://doi.org/10.1111/j.1365-2761.1996.tb00376.x.

Banan Khojasteh, S.M., Sheikhzadeh, F., Mohammadnejad, D., Azami, A., 2009. Histological, histochemical and ultrastructural study of the intestine of rainbow trout (*Oncorhynchus mykiss*). World Appl. Sci. J. 6, 1525–1531.

Bankaitis, E.D., Ha, A., Kuo, C.J., Magness, S.T., 2018. Reserve stem cells in intestinal homeostasis and injury. J. Gastroenterol. 155, 1348–1361. https://doi.org/10.1053/j.gastro.2018.08.016.

Barker, N., 2013. Adult intestinal stem cells: Critical drivers of epithelial homeostasis and regeneration. Nat. Publ. Gr. 15, 19–33. https://doi.org/10.1038/nrm3721.

Barker, N., Van Es, J.H., Kuipers, J., Kujala, P., Van Den Born, M., Cozijnsen, M., Haegebarth, A., Korving, J., Begthel, H., Peters, P.J., Clevers, H., 2007. Identification of stem cells in small intestine and colon by marker gene Lgr5. Nature 449, 1003–1007. https://doi.org/10.1038/nature06196.

Barker, N., Van De Wetering, M., Clevers, H., 2008. The Intestinal Stem Cell, pp. 1856–1864. https://doi.org/10.1101/gad.1674008.1856.

Beumer, J., Clevers, H., 2020. Cell fate specification and differentiation in the adult mammalian intestine. Nat. Rev. Mol. Cell Biol. https://doi.org/10.1038/s41580-020-0278-0.

Bjørgen, H., Li, Y., Kortner, T.M., Krogdahl, Å., Koppang, E.O., 2020. Anatomy, immunology, digestive physiology and microbiota of the salmonid intestine: knowns and unknowns under the impact of an expanding industrialized production. Fish Shellfish Immunol. 107, 172–186. https://doi.org/10.1016/j.fsi.2020.09.032.

Blaufuss, P.C., Bledsoe, J.W., Gaylord, T.G., Sealey, W.M., Overturf, K.E., Powell, M.S., 2020. Selection on a plant-based diet reveals changes in oral tolerance, microbiota and growth in rainbow trout (*Oncorhynchus mykiss*) when fed a high soy diet. Aquaculture 525, 735287. https://doi.org/10.1016/j.aquaculture.2020.735287.

Bohin, N., Keeley, T.M., Carulli, A.J., Walker, E.M., Carlson, E.A., Gao, J., Aifantis, I., Siebel, C.W., Rajala, M.W., Myers, M.G., Jones, J.C., Brindley, C.D., Dempsey, P.J., Samuelson, L.C., 2020. Rapid crypt cell remodeling regenerates the intestinal stem cell niche after notch inhibition. Stem Cell Reports. https://doi.org/10.1016/j.stemcr.2020.05.010.

Bruni, L., Secci, G., Husein, Y., Faccenda, F., Lira de Medeiros, A.C., Parisi, G., 2021. Is it possible to cut down fishmeal and soybean meal use in aquafeed limiting the negative effects on rainbow trout (*Oncorhynchus mykiss*) fillet quality and consumer acceptance? Aquaculture 543, 736996. https://doi.org/10.1016/j.aquaculture.2021.736996.

Cardinaletti, G., Di Marco, P., Daniso, E., Messina, M., Donadelli, V., Finoia, M.G., Petochi, T., Fava, F., Faccenda, F., Cont, M., Cerri, R., Volpatti, D., Bulfon, C., Mandich, A., Longobardi, A., Marino, G., Pulido-rodriguez, L.F., Parisi, G., Tibaldi, E., 2022. Growth and welfare of rainbow trout (*Oncorhynchus mykiss*) in response to graded levels of insect and poultry by-product meals in fishmeal-free diets. Animals 12, 1698. https://doi.org/10.3390/ani12131698.

Chen, M.-S., Lo, Y.-H., Butkus, J., Zou, W., Tseng, Y.-J., Jen, H.-I., Patel, S., Groves, A., Estes, M., Sahin, E., Frey, M., Dempsey, P., Shroyer, N., 2018. Gfi1-expressing Paneth cells revert to stem cells following intestinal injury. bioRxiv. https://doi.org/10.1101/364133.

Elia, A.C., Capucchio, M.T., Caldaroni, B., Magara, G., Dörr, A.J.M., Biasato, I., Biasibetti, E., Righetti, M., Pastorino, P., Prearo, M., Gai, F., Schiavone, A., Gasco, L., 2018. Influence of Hermetia illucens meal dietary inclusion on the histological traits, gut mucin composition and the oxidative stress biomarkers in rainbow trout (*Oncorhynchus mykiss*). Aquaculture 496, 50–57. https://doi.org/10.1016/j.aquaculture.2018.07.009.

Folch, J., Lees, M., Sloane Stanley, G.H., 1957. A simple method for the isolation and purification of total lipides from animal tissues. J. Biol. Chem. 226, 497–509. https://doi.org/10.1016/s0021-9258(18)64849-5.

Forsthoefel, David J., Park, Amanda E., P.A.N, 2011. Stem cell-based growth, regeneration, and remodeling of the planarian intestine. Dev. Biol. 23, 445–459. https://doi.org/10.1016/j.ydbio.2011.05.669.Stem.

Gaudioso, G., Marzorati, G., Faccenda, F., Weil, T., Lunelli, F., Cardinaletti, G., Marino, G., Olivotto, I., Parisi, G., Tibaldi, E., Tuohy, K.M., Fava, F., 2021. Processed animal proteins from insect and poultry by-products in a fish meal-free diet for rainbow trout: impact on intestinal microbiota and inflammatory markers. Int. J. Mol. Sci. 22, 1–26. https://doi.org/10.3390/ijms22115454.

Gehart, H., Clevers, H., 2019. Tales from the crypt: new insights into intestinal stem cells. Nat. Rev. Gastroenterol. Hepatol. 16, 19–34. https://doi.org/10.1038/s41575-018-0081-y.

Giorgini, E., Randazzo, B., Gioacchini, G., Cardinaletti, G., Vaccari, L., Tibaldi, E., Olivotto, I., 2018. New insights on the macromolecular building of rainbow trout (*O. mykiss*) intestine: FTIR imaging and histological correlative study. Aquaculture 497, 1–9. https://doi.org/10.1016/j.aquaculture.2018.07.032.

Greicius, G., Kabiri, Z., Sigmundsson, K., Liang, C., Bunte, R., Singh, M.K., Virshup, D.M., 2018. PDGFRα+ pericryptal stromal cells are the critical source of Wnts and RSPO3 for murine intestinal stem cells in vivo. Proc. Natl. Acad. Sci. U. S. A. 115, E3173–E3181. https://doi.org/10.1073/pnas.1713510115.

Guo, Mingzhang, Breslin, Jerome W., Wu, Mack H., Gottardi, Cara J., S.Y.Y, 2014. Differentiated Troy+ chief cells act as "reserve" stem cells to generate all lineages of the stomach epithelium. Cell 23, 1–7. https://doi.org/10.1016/j.cell.2013.09.008.

Hageman, J.H., Heinz, M.C., Kretzschmar, K., van der Vaart, J., Clevers, H., Snippert, H.J.G., 2020. Intestinal regeneration: regulation by the microenvironment. Dev. Cell 4, 435–446. https://doi.org/10.1016/j.devcel.2020.07.009.

Hamidian, G., Zirak, K., Sheikhzadeh, N., Khani Oushani, A., Shabanzadeh, S., Divband, B., 2018. Intestinal histology and stereology in rainbow trout (*Oncorhynchus mykiss*) administrated with nanochitosan/zeolite and chitosan/zeolite composites. Aquac. Res. 49, 1803–1815. https://doi.org/10.1111/are.13634.

Heijmans, J., Lidth, Van, de Jeude, J.F., Koo, B.K., Rosekrans, S.L., Wielenga, M.C.B., Van De Wetering, M., Ferrante, M., Lee, A.S., Onderwater, J.J.M., Paton, J.C., Paton, A.W., Mommaas, A.M., Kodach, L.L., Hardwick, J.C., Hommes, D.W., Clevers, H., Muncan, V., Van Den Brink, G.R., 2013. ER stress causes rapid loss of intestinal epithelial stemness through activation of the unfolded protein response. Cell Rep. 3, 1128–1139. https://doi.org/10.1016/j.celrep.2013.02.031.

Jacob, J., Di Carlo, S.E., Stzepourginski, I., Benabid, A., Nigro, G., Peduto, L., Jacob, J., Di Carlo, S.E., Stzepourginski, I., Lepelletier, A., Ndiaye, P.D., 2022. Article PDGFR a -induced stromal maturation is required to restrain postnatal intestinal epithelial stemness and promote defense mechanisms ll ll PDGFR a -induced stromal maturation is required to restrain postnatal intestinal epithelial stemness and prom. Stem Cells 29, 856–868.e5. https://doi.org/10.1016/j.stem.2022.04.005.

Krogdahl, Å., Bakke-Mckellep, A.M., B.G, 2003. Effects of graded levels of standard soybean meal on intestinal structure, mucosal enzyme activities, and pancreatic response in Atlantic salmon (*Salmo salar L.*). Aquac. Nutr. 9, 361–371. https://doi.org/10.1016/0022-0248(86)90160-0.

Krogdahl, Å., Gajardo, K., Kortner, T.M., Penn, M., Gu, M., Berge, G.M., Bakke, A.M., 2015. Soya saponins induce enteritis in Atlantic Salmon *(Salmo salar L.*). J. Agric. Food Chem. 63, 3887–3902. https://doi.org/10.1021/jf506242t.

Li, L., Xie, T., 2005. Stem cell niche: structure and function. Annu. Rev. Cell Dev. Biol. 21, 605–631. https://doi.org/10.1146/annurev.cellbio.21.012704.131525.

Li, N., Clevers, H., 2010. Coexistence of quiescent and active adult stem cells in mammals. Science 327, 542–545. https://doi.org/10.1126/science.1180794.

Li, Y., Kortner, T.M., Chikwati, E.M., Munang'andu, H.M., Lock, E.J., Krogdahl, Å., 2019. Gut health and vaccination response in pre-smolt Atlantic salmon (*Salmo salar*) fed black soldier fly (*Hermetia illucens*) larvae meal. Fish Shellfish Immunol. 86, 1106–1113. https://doi.org/10.1016/j.fsi.2018.12.057.

Liu, Y., Chen, Y.G., 2020. Intestinal epithelial plasticity and regeneration via cell dedifferentiation. Cell Regen. 9, 1–11. https://doi.org/10.1186/s13619-020-00053-5.

Mei, X., Gu, M., Li, M., 2020. Plasticity of Paneth cells and their ability to regulate intestinal stem cells. Stem Cell Res Ther 11, 1–13. https://doi.org/10.1186/s13287-020-01857-7.

Nicolás, V.R., Allaire, J.M., Alfonso, A.B., Gómez, D.P., Pomerleau, V., Giroux, V., Boudreau, F., Perreault, N., 2021. Altered mucus barrier integrity and increased susceptibility to colitis in mice upon loss of telocyte bone morphogenetic protein signalling. Cells 10, 2954. https://doi.org/10.3390/cells10112954.

NRC, 2011. Nutrient Requirements of Fish and Shrimp. The National Academies Press, Washington, DC. https://doi.org/10.17226/13039.

Ohara, T.E., Colonna, M., Stappenbeck, T.S., 2022. Adaptive differentiation promotes intestinal villus recovery. Dev. Cell 57, 166–179.e6. https://doi.org/10.1016/j.devcel.2021.12.012.

Ostaszewska, T., Kamaszewski, M., Grochowski, P., Dabrowski, K., Verri, T., Aksakal, E., Szatkowska, I., Nowak, Z., Dobosz, S., 2010. The effect of peptide absorption on PepT1 gene expression and digestive system hormones in rainbow trout (*Oncorhynchus mykiss*). Comp. Biochem. Physiol. - A Mol. Integr. Physiol. 155, 107–114. https://doi.org/10.1016/j.cbpa.2009.10.017.

Pentinmikko, N., Katajisto, P., 2020. The role of stem cell niche in intestinal aging. Mech. Ageing Dev. 191, 111330 https://doi.org/10.1016/j.mad.2020.111330.

Pérez-Pascual, D., Pérez-Cobas, A.E., Rigaudeau, D., Rochat, T., Bernardet, J.-F., Skiba-Cassy, S., Marchand, Y., Duchaud, E., Ghigo, J.-M., 2021. Sustainable plant-based diets promote rainbow trout gut microbiota richness and do not alter resistance to bacterial infection. Anim. Microbiome 3, 47. https://doi.org/10.1186/s42523-021-00107-2.

Polakof, S., Soengas, J.L., 2013. Evidence of sugar sensitive genes in the gut of a carnivorous fish species. Comp. Biochem. Physiol. B Biochem. Mol. Biol. 166, 58–64. https://doi.org/10.1016/j.cbpb.2013.07.003.

Randazzo, B., Zarantoniello, M., Gioacchini, G., Cardinaletti, G., Belloni, A., Giorgini, E., Faccenda, F., Cerri, R., Tibaldi, E., Olivotto, I., 2021. Physiological response of rainbow trout (*Oncorhynchus mykiss)* to graded levels of Hermetia illucens or poultry by-product meals as single or combined substitute ingredients to dietary plant proteins. Aquaculture 538, 736550. https://doi.org/10.1016/j.aquaculture.2021.736550.

Refstie, S., Korsøen, Ø.J., Storebakken, T., Baeverfjord, G., Lein, I., Roem, A.J., 2000. Differing nutritional responses to dietary soybean meal in rainbow trout (*Oncorhynchus mykiss*) and Atlantic salmon (*Salmo salar)*. Aquaculture 190, 49–63. https://doi.org/10.1016/S0044-8486(00)00382-3.

Romano, A., Barca, A., Storelli, C., Verri, T., 2014. Teleost fish models in membrane transport research: the PEPT1(SLC15A1) H+-oligopeptide transporter as a case study. J. Physiol. 592, 881–897. https://doi.org/10.1113/jphysiol.2013.259622.

Seibel, H., Chikwati, E., Schulz, C., Rebl, A., 2022. A multidisciplinary approach evaluating soybean meal-induced enteritis in rainbow trout (*Oncorhynchus mykiss*). Fishes 7, 1–18. https://doi.org/10.3390/fishes7010022.

Shoshkes-Carmel, M., Wang, Y.J., Wangensteen, K.J., Tóth, B., Kondo, A., Massassa, E.E., Itzkovitz, S., Kaestner, K.H., 2018. Subepithelial telocytes are an important source of Wnts that supports intestinal crypts. Nature 557, 242–246. https://doi.org/10.1038/s41586-018-0084-4.

Silva, P.F., McGurk, C., Knudsen, D.L., Adams, A., Thompson, K.D., Bron, J.E., 2015. Histological evaluation of soya bean-induced enteritis in Atlantic salmon (*Salmo salar L.*): quantitative image analysis vs. semi-quantitative visual scoring. Aquaculture 445, 42–56. https://doi.org/10.1016/j.aquaculture.2015.04.002.

Tata, P.R., Mou, H., Pardo-Saganta, A., Zhao, R., Prabhu, M., Law, B.M., Vinarsky, V., Cho, J.L., Breton, S., Sahay, A., Medoff, B.D., Rajagopal, J., 2013. Dedifferentiation of committed epithelial cells into stem cells in vivo. Nature 503, 218–223. https://doi.org/10.1038/nature12777.

Terova, G., Corà, S., Verri, T., Rimoldi, S., Bernardini, G., Saroglia, M., 2009. Impact of feed availability on PepT1 mRNA expression levels in sea bass (*Dicentrarchus labrax*). Aquaculture 294, 288–299. https://doi.org/10.1016/j.aquaculture.2009.06.014.

Terova, G., Robaina, L., Izquierdo, M., Cattaneo, A.G., Molinari, S., Bernardini, G., Saroglia, M., 2013. PepT1 mRNA expression levels in sea bream (*Sparus aurata)* fed different plant protein sources. Springerplus 2, 1–14. https://doi.org/10.1186/2193-1801-2-17.

Tetteh, P.W., Basak, O., Farin, H.F., Wiebrands, K., Kretzschmar, K., Begthel, H., Van Den Born, M., Korving, J., De Sauvage, F., Van Es, J.H., Van Oudenaarden, A., Clevers, H., 2016. Replacement of lost Lgr5-positive stem cells through plasticity of their enterocyte-lineage daughters. Cell Stem Cell 18, 203–213. https://doi.org/10.1016/j.stem.2016.01.001.

Tibaldi, E., Chini Zittelli, G., Parisi, G., Bruno, M., Giorgi, G., Tulli, F., Venturini, S., Tredici, M.R., Poli, B.M., 2015. Growth performance and quality traits of European sea bass (*D. labrax)* fed diets including increasing levels of freeze-dried Isochrysis sp. (T-ISO) biomass as a source of protein and n-3 long chain PUFA in partial

substitution of fish derivatives. Aquaculture 440, 60–68. https://doi.org/10.1016/j.aquaculture.2015.02.002.

Van Es, J.H., Sato, T., Van De Wetering, M., Lyubimova, A., Yee Nee, A.N., Gregorieff, A., Sasaki, N., Zeinstra, L., Van Den Born, M., Korving, J., Martens, A.C.M., Barker, N., Van Oudenaarden, A., Clevers, H., 2012. Dll1 + secretory progenitor cells revert to stem cells upon crypt damage. Nat. Cell Biol. 14, 1099–1104. https://doi.org/10.1038/ncb2581.

Venold, F.F., Penn, M.H., Krogdahl, Å., Overturf, K., 2012. Severity of soybean meal induced distal intestinal inflammation, enterocyte proliferation rate, and fatty acid binding protein (Fabp2) level differ between strains of rainbow trout (*Oncorhynchus mykiss)*. Aquaculture 364–365, 281–292. https://doi.org/10.1016/j.aquaculture.2012.08.035.

Venold, F.F., Penn, M.H., Thorsen, J., Gu, J., Kortner, T.M., Krogdahl, Å., Bakke, A.M., 2013. Intestinal fatty acid binding protein (fabp2) in Atlantic salmon (*Salmo salar*): localization and alteration of expression during development of diet induced enteritis. Comp. Biochem. Physiol. - A Mol. Integr. Physiol. 164, 229–240. https://doi.org/10.1016/j.cbpa.2012.09.009.

Verdile, N., Mirmahmoudi, R., Brevini, T.A.L., Gandolfi, F., 2019. Evolution of pig intestinal stem cells from birth to weaning. Animal 3, 1–10. https://doi.org/10.1017/S1751731119001319.

Verdile, N., Pasquariello, R., Brevini, T.A.L., Gandolfi, F., 2020a. The 3d pattern of the rainbow trout (*Oncorhynchus mykiss*) enterocytes and intestinal stem cells. Int. J. Mol. Sci. 21, 1–30. https://doi.org/10.3390/ijms21239192.

Verdile, N., Pasquariello, R., Scolari, M., Scirè, G., Brevini, T.A.L., Gandolfi, F., 2020b. A detailed study of rainbow trout (*Onchorhynchus mykiss*) intestine revealed that digestive and absorptive functions are not linearly distributed along its length. Animals 10, 745. https://doi.org/10.3390/ani10040745.

Verdile, N., Pasquariello, R., Cardinaletti, G., Emilio, Tibaldi, Brevini Tiziana, A.L., G.F., 2022. Telocytes: active players in the rainbow trout (*Oncorhynchus mykiss*) intestinal stem-cell niche. Animals. 12 (1), 74. https://doi.org/10.3390/ani12010074.

Wang, J., Yan, X., Lu, R., Meng, X., Nie, G., 2017. Peptide transporter 1 (PepT1)in fish: a review. Aquac. Fish. 5, 193–206. https://doi.org/10.1016/j.aaf.2017.06.007.

Wenzel, U., Meissner, B., Döring, F., Daniel, H., 2001. PEPT1-mediated uptake of dipeptides enhances the intestinal absorption of amino acids via transport system b 0,+. J. Cell. Physiol. 186, 251–259. https://doi.org/10.1002/1097-4652(200102)186:2<251::AID-JCP1027>3.0.CO;2-F.